Ana Fernández-Barquín[1,*]
Clara Casado-Coterillo[1]
Miren Etxeberria-Benavides[2]
Jon Zuñiga[2]
Angel Irabien[1]

Comparison of Flat and Hollow-Fiber Mixed-Matrix Composite Membranes for CO_2 Separation with Temperature

Zeolite A/poly (1-trimethylsilyl-1-propyne) (zeoliteA/PTMSP) and [emim][Ac]/chitosan (IL/CS) are mixed-matrix membrane (MMM) materials with enhanced CO_2/N_2 permselectivity even at higher temperature. The scalability to asymmetric flat and hollow-fiber geometry by a simple dip-coating method was analyzed. The CO_2/N_2 separation performance was evaluated at different temperatures. The resulting composite membranes exhibit a significantly enhanced CO_2 permeation flux because the MMM layer thickness is reduced by 97 % from flat to hollow-fiber geometries in IL-CS composite membranes, while the selectivity is maintained similar to the self-standing membranes, thus proving that compatibility between the membrane component materials leads to a defect-free composite membrane, regardless the geometry and temperature.

Keywords: CO_2 capture, High permeance, Mixed-matrix composite membranes, Post-combustion capture

Received: October 24, 2016; *revised:* February 13, 2017; *accepted:* February 21, 2017

DOI: 10.1002/ceat.201600580

1 Introduction

Post-combustion technology is the strategy with the greatest near-term potential in the CO_2 capture [1]. The research on membrane technology as a potential alternative option in post-combustion CO_2 capture has focused on two main lines: membrane material development and membrane engineering of the separation process.

Polymers are the most developed materials in CO_2 membrane material development. Despite the outcome of several commercial polymeric membranes, these are not yet an alternative to conventional technologies for the CO_2 postcombustion capture at industrial-scale facilities, due to the lack of productivity and separation selectivity [2]. This makes necessary a large number of membrane modules to provide the membrane area that could treat the large volume of flue gas in post-combustion processes, which requires higher investment [3].

Mixed-matrix membranes (MMMs) combine the molecular sieving properties of inorganic fillers with the processability of polymers to achieve a new hybrid homogeneous material with synergic mechanical and functional properties [4, 5]. Material selection for both polymer and fillers is a crucial aspect in the synthesis of MMMs [6].

For practical applications, membranes with high permselectivity and high thermal and mechanical stability are required. Synthesis of high-flux membranes with an asymmetric structure and the development of composite membranes may make membrane technology competitive with other conventional CO_2 capture technologies [7]. Asymmetric membranes can be comprised of an integrally skin layer generated on a porous support of the same material, or composite membranes with a defect-free top thin dense layer on a porous support layer that is usually made of a different material [8]. A polymeric membrane with asymmetric structure is the most preferred material for industrial membrane-based gas separation applications [9].

The performance of a membrane separator for gas separation depends not only on permeability and selectivity, but also on membrane geometrical structure since processing membrane materials into practical geometries is as important as developing new membrane materials [10]. Asymmetric flat membranes where the costly CO_2-selective materials are coated as a thin layer on top of a robust, more economic support are a first step of the development. Moreover, the hollow-fiber (HF) membrane configuration allows a larger effective membrane area per module volume which results in greater process intensification and scalability [11].

Composite HF membranes (CHFs) for CO_2 capture have been prepared by dip-coating as a more scalable way than spinning to obtain a thin layer of a permselective material on top of a processable, economic HF support [12]. This needs careful

[1]Ana Fernández-Barquín, Dr. Clara Casado-Coterillo, Dr. Angel Irabien
fbarquina@unican.es
Universidad de Cantabria, Department of Chemical and Biomolecular Engineering, Av. Los Castros s/n, 39005 Santander, Spain.

[2]Miren Etxeberria-Benavides, Jon Zuñiga
Tecnalia Research and Innovation, Energy and Environmental Division, Pasealekua 2, 20009 Donostia-San Sebastián, Spain.

consideration of the porosity and pore size of the support to avoid penetration and minimize resistance to gas transport [8, 9, 11].

Poly(1-trimethylsilyl-1-propyne) (PTMSP) has gained attention in the last decades because it is the polymer with the highest reported permeability in spite of its glassy structure which leads to a low chain mobility and high glass transition temperature > 523 K, which makes it resistant at elevated temperatures [13]. Its high permeability comes with low ideal selectivity and decreases with time due to physical aging because of the relaxation of its large free volume, and, sometimes, chemical aging due to oxidation of the double bonds in the chain backbone [13, 14]. Efforts to limit physical aging have been addressed by MMMs and asymmetric configuration. In a previous work, the compatibility between fillers and PTMSP has been addressed by using porous zeolites, porous crystalline aluminosilicates whose Si/Al ratio can be tuned up to enhance PTMSP performance [15], while hardly influencing the uptake of CO_2 [16].

Chitosan (CS) is the deacetylated derivative from chitin, an abundant biodegradable natural polymer, cheap, and obtained from renewable sources. For the separation of CO_2 from flue gas effluents that contain water vapor, CS-based membranes have been studied using water as fixed carrier for CO_2 and water permeation, and the transport mechanism, i.e., solution diffusion + facilitated transport, has started to be investigated. The mechanical properties of CS are still a main drawback and authors have attempted to enhance the resistance by crosslinking, coating on a porous support, surface modification, and interfacial polymerization of a polyamide/CS blend on a polyethersulfone (PES) porous ultrafiltration (UF) membrane to improve stability [17].

Ionic liquids (ILs) possess both cation and anion parts and have been studied both as supported IL membranes and MMMs to enhance gas separation performance and mechanical resistance [18]. In a previous work, we have explored the hybridization effect of CS by introducing of 5 wt % 1-ethyl-3-methylimidazolium acetate, [emim][Ac], a highly CO_2-absorbing and nontoxic IL, which improved slightly the selectivity of pure CS membranes and removed the effect of temperature on CO_2/N_2 separation performance, thus giving scope for operating at temperatures up to 323 K [19].

The reports on MMMs have been mostly focused on dense flat homogeneous morphologies at a single temperature and pressure, and the advantages gave scope to an abundant literature [5]. Carruthers et al. explored the effect of the change of geometry on integrally skinned polymer membranes from dense to HF geometry [20]. MMMs in HF configuration have also been studied at laboratory scale for different polymer/filler combinations and dual-layer spinning processes [21], but still the formation mechanism is not well-known [22] and a completely dense (defect-free) selective layer is necessary to keep the selectivity of the material [23], usually needing caulking with silicone rubber [9, 24, 25].

In our previous works, we have investigated the performance of MMMs made from highly CO_2-selective and permeable materials that overcome the Robeson upper bound [26] in self-standing configuration, in two approaches: (i) the selectivity and aging resistance of PTMSP has been improved by adding small-pore zeolites of varying Si/Al ratio [15] and topology [27], and (ii) the thermal and mechanical resistance and selectivity of CS biopolymer has been improved by adding [emim][Ac] [19], microporous titanosilicate ETS-10 [28], and ZIF-8 and HKUST-1 nanoparticles [29]. The effect of temperature on CO_2/N_2 separation has been studied in the range 298–333 K and the highest CO_2/N_2-permselective membrane materials were selected in this work to fully explore the effect of the change of geometry on membrane performance.

Therefore, the goal of the present work is to study the change of geometry of CO_2-permselective and thermally resistant MMM self-standing materials as the coating layers on flat and HF polymer-compatible supports, taking into account the reduction of selective layer thickness and influence of temperature to keep the high permselectivity and thermal stability in advanced membrane configurations. Membranes were characterized by field electron scanning microscopy (FE-SEM) and N_2 and CO_2 permeation in the temperature range 298–333 K. The comparison of the performance of dense homogeneous flat, composite flat membranes, and composite HFs prepared and characterized under the same conditions enables analysis of the influence of geometry and temperature on membrane behavior.

2 Experimental

2.1 Membrane Preparation

2.1.1 Dense Membranes

Dense homogeneous flat membranes were synthesized by solution casting as reported in previous works [15, 29]. For PTMSP-based membranes, PTMSP (Gelest) was dissolved in toluene in a 1.5 wt % polymer solution, for one day at 333 K, before being dried at 343 K to remove possible impurities. The zeolites were dried at 373 K for several hours, then dispersed in the solvent for 2 h before adding the polymer solution. The nominal zeolite loading employed was 20 wt % to the PTMSP polymer ratio. The films were cast on glass Petri dishes and dried slowly at ambient conditions. Finally, the membranes were immersed in methanol for 5 min before the gas permeation tests, since this was the method that prevailed to assure that all PTMSP-based membranes were in similar initial conditions and thus guarantee reproducible permeation results [15].

For the CS-based membranes, the procedure was similar [29]. CS 1.5 wt % was first dissolved in 2 wt % acetic acid (glacial; Panreac) aqueous solutions by stirring at 353 K for 24 h under reflux. The obtained solution was then filtered to remove possible impurities. After this step, the IL 1-ethyl-3-methylimidazolium acetate (97 wt %; Sigma Aldrich) was added in 5 wt % proportion with respect to the CS concentration in the solution. For the preparation of HKUST-1/IL-CS membranes, the HKUST-1 nanoparticle fillers were first stirred in 2 mL of deionized water before being added to the IL-CS solution in 5 wt % loading with respect to the total IL-CS organic composition.

The dried membranes were removed from the Petri dish, neutralized in 1 M NaOH, and rinsed with abundant distilled

water before permeation experiments in order to ion-exchange the NH_3^+ functional groups of the polymer matrix [19, 29]. As the IL is in a very small proportion, i.e., 5 wt % to the total amount of solid membrane, it is not expected to be in the liquid form, but as a sort of binder between chains or nanoparticles as observed in previous works [28, 29].

The fillers used were zeolite A, with Si/Al = 1 (molecular sieves 4 Å; Aldrich) and an average particle size of 2.5 μm, nanometer-sized HKUST-1 particles (with an average particle size of 0.34 μm prepared by a procedure as described in [29], and the highly CO_2-absorbing [emim][Ac] (97 %; Aldrich), which had proved to enhance the CO_2/N_2 selectivity of the IL-CS hybrid membranes as well as the thermal and mechanical stability [19].

2.1.2 Composite Flat Membranes

Flat supports made of PES were purchased from PALL Corp. (USA) with porosities of 0.1 μm. A selected volume of the casting polymeric or hybrid solution was degassed in the ultrasound bath (SELECTA, Spain) for 10 min before coating the porous support.

For the preparation of asymmetric MMMs, the compositions were selected among the most CO_2/N_2-permselective membrane materials from the dense membranes studied previously: 5 wt % HKUST-1/IL-CS/PES and 20 wt % zeoliteA-PTMSP/PES. Composite PTMSP/PES membrane was also prepared for comparison. In general, a known volume of the coating solution was cast on top of the PES support and allowed to dry slowly under ambient conditions, then removed from the glass plates when dried, similarly to the dense homogeneous flat membranes described above.

CS-based asymmetric membranes were prepared by a modified method after the interfacial polymerization (IP) reported to correct imperfections on the coating of semi-crystalline polymer composite membranes on porous polymer supports, although the uniformity of the skin layer thickness is difficult to control by this method [30, 31]. In this work, a modified IP method was used to prepare the CS and IL-CS composite membranes to avoid the formation of scales that appeared by simple coating. In this procedure, the organic phase, consisting of *n*-hexane with 0.1 % (m/m) of trimesoyl chloride (TMC), was first deposited on the support and, after drying at 323 K for 10 min, the hydrophilic phase composed of CS solution was coated over the other. The membrane was dried at room temperature for 48 h prior to a final drying step at 323 K for 90 min before characterization.

2.1.3 Composite Hollow-Fiber Membranes

Likewise, the same compositions accounting for the best selective membranes were used to prepare composite HF membranes by dip-coating. The HF supports selected were polysulfone (PSf) for the CS-based membranes and P84 for the PTMSP-based membranes, because of compatibility issues that will be discussed later. Both PSf and P84 HF supports were prepared at Tecnalia by conventional spinning techniques [32]. As in the composite flat MMMs, the composite HF membranes were prepared by coating the selective solution, i.e., PTMSP, 20 wt % zeolite A/PTMSP, IL-CS, and 5 wt % HKUST-1/IL-CS, respectively, on the outer side of the HF support, with the extremes covered to prevent penetration in the lumen side. The HF supports were immersed in the selective coating solution for 60 s. The CHF membranes were dried for at least 24 h under the same conditions as the flat membranes, i.e., slow evaporation in fume-hood at room temperature, before they were subjected to a second coating. At this point, the number of coatings was studied for the first CHF, i.e., IL-CS-based membranes, observing that two coatings were necessary to obtain a smooth regular layer thickness. Finally, the composite HF membranes were dried for another 48 h at least, before testing the gas permeation performance.

2.2 Membrane Characterization

The pure gas permeance was measured using the experimental setup described previously [27], where a differential transducer (Omega, UK) measured the pressure difference between the feed and permeate sides, in order to determine the gas volume flowing through the membrane. The module is placed in a thermostatic bath in order to operate under isothermal conditions. The permeation cell, in the case of flat membranes, is composed of two stainless-steel compartments that are pneumatically pressed to each other by a Viton ring sealing the membrane. The effective flat membrane area is 15.55 cm^2. The composite HF membranes were sealed in 1/8-inch tubing using an epoxy resin adhesive [33], and placed in a stainless-steel permeation module. The effective length of the fiber was 20 cm, giving an effective area of 2.16 cm^2.

Gas permeation tests were carried out at a temperature range of 298–333 K. The gases were fed at 3 bar and the permeate was evacuated to create the pressure difference through the membrane.

A commonly accepted unit for gas permeability is the Barrer, where 1 Barrer = $(cm^3(STP)\,cm)/(cm^2 s\,cmHg) \times 10^{-10}$. When the thickness is difficult to define, as is the case with asymmetric membranes, the pressure-normalized flux, or permeance ($J^{1)} = P_i/l$), is used instead. In this case, the gas permeation unit (GPU) is usually employed, defined as $1\,GPU = 10^{-6}\,(cm^3(STP))/(cm^2 s\,cmHg)$. The permeance ratio determines the selectivity of the separation for a component in a binary mixture:

$$\alpha = \frac{\left(P/l\right)_{CO2}}{\left(P/l\right)_{N2}} \tag{1}$$

The membrane thickness of the dense homogeneous films and the overall thickness of composite flat membranes were determined by means of a digital micrometer (Mitutoyo digimatic micrometer, IP 65) whose precision is up to 0.001 mm.

1) List of symbols at the end of the paper.

The thickness of a defect-free composite membrane, i.e., membranes exhibiting near-intrinsic selectivity, is usually calculated from the ratio of the permeance of the asymmetric membrane and the permeability of the dense homogeneous film made of the same material, as follows [8, 9]:

$$l = \frac{P(\text{dense film})}{J(\text{asymmetric membrane})} \quad (2)$$

The cross-sectional area and morphology of selected membranes of each composition of the selective layer were observed by field electron scanning electron microscopy in the FE-SEM Carl Zeiss MERLIN™ equipment of the Universidad de Zaragoza. Sample specimens were prepared by freezing in liquid nitrogen before fracturing and sputtering with gold prior to observation. This allows observing the thickness of the selective layer of composite membranes, and comparison with Eq. (2) allows estimating the quality of the coating. In the case of the HF membranes and supports, two specimens were cut, from the top and bottom parts of the length of the fiber.

The viscosities of the solutions were measured at different temperatures using a rotational viscometer (Smart Series, Fungilab, Spain) with a shear rate of 20–100 rpm.

3 Results and Discussion

In this work, more permeable materials were used in the coated layer than the support with the aim to obtain a higher production rate of CO_2 while keeping the same value of CO_2/N_2 selectivity of the coating materials as in dense film configuration [10]. Permeability data through PTMSP, 20 wt % zeolite A/PTMSP, IL-CS, and HKUST-1/IL-CS unsupported membranes obtained in our laboratory have been previously reported [15, 29].

The permeance of CO_2 and N_2 through the porous PES (flat), PSf (HF), and P84 (HF) supports employed in this work at 298 K are presented in Tab. 1. It can be observed that the supports used in this work are not CO_2-selective and the selectivity is close to the Knudsen selectivity for the CO_2/N_2 gas pair (0.80), which means this is the gas transport mechanism dominating gas transfer through the support that only offers mechanical strength [8] and attributes any differences in permselectivity for the composite membranes' performance to the selective coated layer. Although the permeance through the supports used in this work is lower than some literature values, they are similar to others [8, 9, 12, 34–41], as collected in Tab. 1, probably because of the differences between considered thickness and measurement procedures from one work to another.

When the thin dense layer is prepared from materials with extremely high permeability [36, 42–44] it will be responsible of the molecular separation, while the bulk support layer provides mechanical strength with negligible mass transport resistance [42]. When selecting highly permeable materials as responsible of the transport mechanism to obtain high permeation flux, Kattula et al. [42] observed that the permeance can be enhanced by designing a selective layer with materials with superior permeability of the support, as well as reducing the selective dense layer responsible of the separation mechanism. For the fabrication of thin CHF for CO_2 separation, it is usually necessary to provide a poly(dimethylsiloxane) (PDMS) [45] or PTMSP [46] gutter layer to prevent penetration of the porous support by the selective material of the coated layer.

Table 1. Permeance of CO_2 and N_2 through the porous PES (flat), polysulfone (HF), polyimide (PI), and P84 (HF) supports at 298 K and 3 bar.

Support	J(CO_2) [GPU]	J(N_2) [GPU]	CO_2/N_2
PSf (HF) [8]	3160	4700	0.67
PSF (HF) [12]	1.85	0.37	5.00
PSF (HF) [34]	19.88	–	–
PSF (HF) [35]	78.11	2.27	34.41
PSf (HF) [9]	69.66	18.78	3.71
PES (flat) [36]	235	276	0.85
PES (HF)[37]	–	1.6	–
P84 (HF) [38]	34	–	–
P84 (HF) [39]	4.9	1.5	3.27
P84 (HF) [40]	1.2	–	–
PI (HF) [41]	80	–	–
PES (flat) (this work)	12 ± 1.5	8 ± 0.6	1.5 ± 0.74
PSf (HF) (this work)	20 ± 2.8	17 ± 0.7	1.17 ± 0.18
P84 (HF) (this work)	40 ± 3.1	28 ± 0.5	1.43 ± 0.67

Considering the viscosity of the coating solution is essential to obtain a defect-free thin selective layer over all the support, especially in HF membrane geometry since it is important that the coating is homogeneously distributed not only on the perimeter of the fiber but also along the whole length [47, 48]. The concentration of the coating solution has a significant impact on the ultimate gas separation performance [49]. He et al. [50] reported that at a low concentration of sulfonated polyethersulfone (SPES) in the coating solution, the coating layers completely separate from the PSf support. Lasseuguette et al. [44] showed that the thickness of a Newtonian fluid coating a fiber depends on the viscosity.

In this work, the viscosity of different CS and PTMSP solutions varying the mass concentration of the polymer at different temperatures was investigated. The shear rates were varied from 20 to 100 rpm and the viscosities were independent of the shear rate, which means that the solutions presented a Newtonian behavior. As a result, the values of the viscosities plotted in Fig. 1 were recorded at a shear rate of 100 rpm as a function of polymer mass fraction at different temperatures.

The increase of both CS and PTMSP mass fractions led to an increase of their viscosity following a classical experimental power law, in Eqs. (3) and (4), respectively [44]. As expected, the polymer solution viscosity decreased with rising temperature.

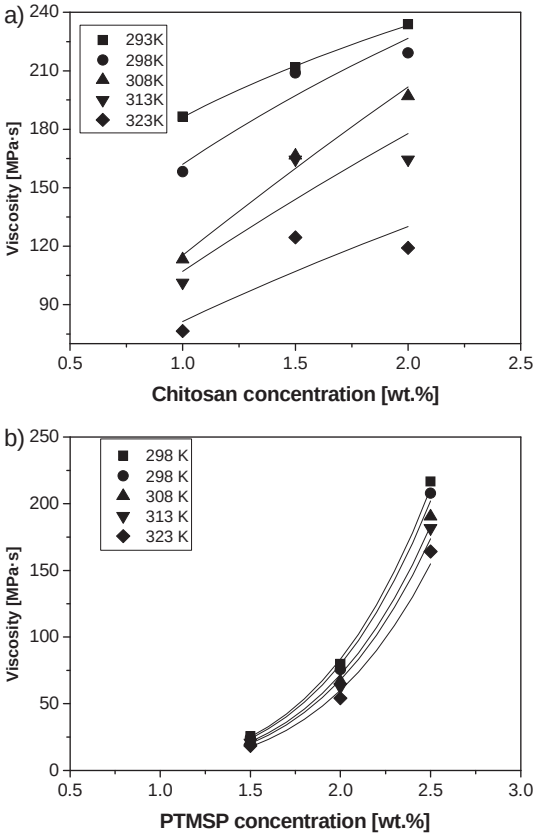

Figure 1. Viscosity of the solutions vs. polymer concentration: (a) CS, (b) PTMSP, and temperature.

$$\eta = 0.0382\exp[\mathrm{CS}]^{7.49\times 10^5 \exp\left(-3.6\times 10^4/8.314T\right)} \quad (3)$$

$$\eta = 0.11\exp\left(9.11\times 10^3/8.314T\right)[\mathrm{PTMSP}]^{4.96\exp\left(-4.2\times 10^2/8.314T\right)} \quad (4)$$

Taking into account the viscosity of the solutions and seeking a compromise between the solution viscosity and the amount of polymer used, the concentrations of CS and PTMSP selected to prepare the coating solutions were 1.5 and 2 wt %, respectively, since PTMSP has a lower viscosity than CS. Besides, the P84 HF support was selected for PTMSP-based CHF membrane preparation for two reasons: (i) to avoid the support to be impregnated by the coating solution given the lower viscosity of the PTMSP-based solutions than those based on CS, since the P84 HF support does not have the voids that are present in the PSf HF structure, and (ii) the apparent collapse or contraption of the PSf HF by plasticization of the polymer after coating with PTMSP-based solutions. This phenomenon could be attributed to a plasticization of the HF support in the presence of toluene that leads to a contraction of the polymer structure. On the other hand, the compatibility between CS and PSf has been reported in literature [51, 52].

Another important factor to be taken into account to obtain a defect-free composite membrane with selectivity close to the intrinsic selectivity of self-standing MMM and higher permeance (because of the lower thickness) was the minimum number of coating steps necessary. With this aim, the effect of the number of coatings of the IL-CS hybrid solution was studied. Fig. 2 shows that one coating with the IL-CS solution in PSf HF support is not enough to cover all the perimeter of the outer surface along the whole length of the fiber, the IL-CS layer being thicker at the bottom than the top of the fiber.

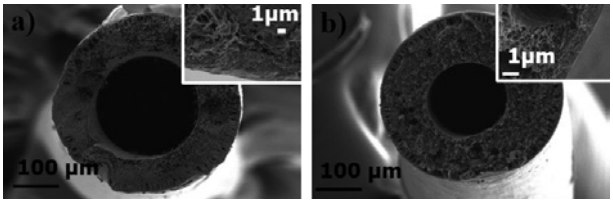

Figure 2. FE-SEM images of IL-CS composite HF membranes with (a) one coating, (b) two coatings. The inset shows a detail of the selective layer.

The permeation data in Tab. 2 also demonstrates that one coating is insufficient to achieve a membrane as selective as the dense homogeneous unsupported IL-CS hybrid membrane [19, 29]. The thickness of the ZIF-8/6FDA-DAM layer coated on 6FDA-DAM HF membrane presented by Zhang et al. [10] has to be at least 7–12 µm to assure adhesion and avoid defects. The apparent thickness given in Tab. 2 was calculated with Eq. (2). The IL-CS-coated layer is homogeneous and well adhered to the PSf HF support. Likewise, two coatings were necessary so that the material covers equally the whole length in CS/PSf CHF membranes [51] and the number of coatings and concentration of the coating solution on the PSf HF support observed a trade-off. Consequently, two coatings were used in the rest of the CHF membranes prepared and discussed further on.

Fig. 3 presents the FE-SEM images of the dense homogeneous flat (left), composite flat (center), and CHF (right) geometries prepared in this work. The IL-CS-based composite membrane morphology revealed a homogeneous dense layer for all the geometries (Fig. 3 a). In Fig. 3 b, the HKUST-1/IL-CS-based membranes are observed. The HKUST-1 nanoparticles were found homogeneously dispersed all along the perimeter of the outer layer of the CHF membrane, and very well dispersed in

Table 2. Influence of coating times with IL-CS hybrid solutions on the properties of composite HF membranes.

Solution concentration [wt %]	Viscosity [cP] (30 °C)	Coating times	Apparent thickness [µm]	J(CO_2) [GPU]	α (CO_2/N_2)
1.5	206.4	1	0.156	3120	1.35
		2	0.53	4226	2.48

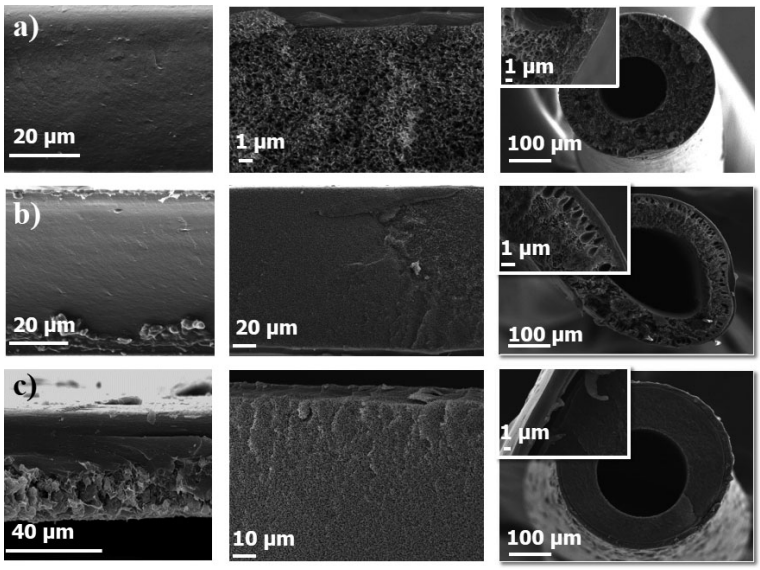

Figure 3. FE-SEM images of the membranes prepared from (a) IL-CS, (b) 5 wt % HKUST-1/IL-CS, (c) 20 wt % zeolite A/PTMSP selective layers. Left, medium, and right columns correspond to dense homogeneous flat, composite flat, and composite HF geometries, respectively. Details of the selective layers are zoomed in the insets.

the selective layer of the composite flat membrane, as the Cu from HKUST-1 was homogeneously distributed throughout the dense IL-CS unsupported membrane [29]. As to the zeolite A/PTMSP-based membranes (Fig. 3 c), the dual layer formation observed in the dense unsupported membranes seemed to be transformed in regularly dispersed circular sockets containing the zeolite A particles in the CHF morphology, as reported by Zhang et al. [10] for the ZIF-8 nanoparticles in 6FDA-DAM HF and attributed by those authors to the aggressive fracturing in liquid nitrogen prior to SEM observation. To improve zeolite dispersion in the PTMSP-based layer, the drying procedure was adapted as similar as possible to the dense homogeneous flat membrane [15] and selectivity was slightly improved, as discussed later.

Tab. 3 gives the selective layer thicknesses of the different membrane configurations studied in this work, both experimentally measured and calculated from Eq. (2) [8, 9]. The selective layer of an asymmetric MMM cannot be thinner than the diameter of a single particle without creating undesirable membrane defects, and a "conceptually feasible" MMM HF should possess minimal skin thickness of < 200–500 nm to enable high permeance and reduced sheath layer thickness of < 1–5 mm and minimize membrane material cost [10].

From the measured values in Tab. 3, it can concluded that the selective layer thickness is reduced by 97 % from flat to HF geometry for the IL-CS-based composite membranes. The layer thicknesses of PTMSP- and zeolite A/PTMSP composite membranes only decreased by 90 % and 85 % from flat to fiber geometry, respectively. The thicknesses of the dense homogeneous self-standing membranes are also given for comparison. The selective layer thickness calculated from Eq. (2) provided more homogeneous values for the IL-CS based composite membranes than for the PTMSP- based composite membranes. This is attributed to higher compatibility between membrane material components in the first case that allows the translation to defect-free MMM composite membranes. This agrees with the calculation of the apparent thicknesses by Eq. (2), where the values of the calculated thickness agree better for the IL-CS-based membranes than for the PTMSP-based membranes, pointing to the presence of pinholes in the latter case [24]. The least square minimum error between the calculated and measured effective thicknesses (not shown) are below 0.1 % and 1.5 % for IL-CS and PTMSP-based membranes, which is attributed to the fact that the Knudsen contribution to the flux appears in the zeolite A/PTMSP composite MMMs due to lower compatibility and apparition of pinholes.

The influence of temperature in the CO_2/N_2 gas separation performance of these membranes was analyzed in terms of single-gas permeance in the range from 298 K to 333 K. The CO_2 permeances as well as the CO_2/N_2 selectivities of the membranes in dense homogeneous flat, composite flat, and CHF geometries are collected in Tab. 4, with an experimental deviation < 15 %. The CO_2 permeance increases significantly for the composite flat and HF geometries with respect to the corresponding dense homogeneous unsupported membrane of the same material. This enhancement is attributed to the reduction of the selective layer thickness shown in Tab. 3.

Table 3. Measured and calculated selective layer thicknesses of the different membranes prepared.

	Measured selective layer thickness [µm]			Calculated effective selective layer thickness [µm]			
Selective membrane material	Dense homogeneous flat	Composite flat	Composite HF	Composite flat (CO_2)	Composite flat (N_2)	Composite HF (CO_2)	Composite HF (N_2)
IL-CS	128 ± 4.0	16.75 ± 8.5	0.53 ± 0.1	13.66 ± 3.26	8.04 ± 1.03	6.5 ± 0.54	4.88 ± 0.51
5 wt % HKUST-1/IL-CS	91.8 ± 2.7	76.55 ± 23.3	1.89 ± 0.5	67.18 ± 15.42	51.94 ± 10.91	36.85 ± 4.9	45.79 ± 12.5
PTMSP	100 ± 31.6	76.15 ± 5.4	7.20 ± 1.7	131.9 ± 40.83	87.25 ± 28.17	306.85 ± 52.2	243.85 ± 59.29
20 wt % zeolite A/PTMSP	98.6 ± 23.6	45.55 ± 9.6	6.93 ± 1.5	57.59 ± 21.24	27.86 ± 13.13	145 ± 29.83	4.1 ± 2.41

Table 4. Dense homogeneous flat, composite flat, and composite HF membranes performance obtained at different temperatures.

		Dense homogeneous flat		Composite flat		Composite HF	
Selective membrane material	T [K]	J (CO_2) [GPU]	α (CO_2/N_2)	J (CO_2) [GPU]	α (CO_2/N_2)	J (CO_2) [GPU]	α (CO_2/N_2)
IL-CS	298	8.49 ± 1.65	2.66 ± 0.85	102.31± 3.22	2.31 ± 0.65	4226.42 ± 92.98	2.48 ± 0.91
	308	9.78 ± 1.79	2.96 ± 0.95	111.28 ± 4.25	2.26 ± 0.41	4533.96 ± 86.71	2.46 ± 0.91
	313	10.28 ± 2.17	3.25 ± 1.13	118.54 ± 2.55	2.32 ± 0.37	5096.23 ± 251.91	2.42 ± 0.84
	323	10.56 ± 2.79	3.04 ± 1.37	123.48 ± 6.96	2.14 ± 0.28	5679.25 ± 425.36	2.31 ± 0.73
5 wt % HKUST-1/ IL-CS	298	48.29 ± 4.32	9.68 ± 2.16	69.20 ± 2.47	3.37 ± 0.46	2244.44 ± 72.14	5.51 ± 0.35
	308	64.91 ± 7.46	11.85 ± 1.47	100.67 ± 10.46	4.39 ± 1.46	2492.59 ± 285.02	5.93 ± 1.98
	313	67.28 ± 9.46	7.20 ± 0.99	106.34 ± 7.56	4.44 ± 0.80	3506.35 ± 223.94	5.49 ± 1.70
	323	85.59 ± 6.49	6.90 ± 1.68	109.86 ± 6.55	3.90 ± 0.85	3186.24 ± 115.97	4.71 ± 1.73
PTMSP	298	180.01 ± 25.51	0.97 ± 0.15	128.56 ± 16.86	0.97 ± 0.16	1129.61 ± 266.34	1.15 ± 0.09
	308	179.30 ± 11.14	0.75 ± 0.14	109.05 ± 4.29	0.90 ± 0.12	1115.48 ± 362.66	1.38 ± 0.12
	313	160.62 ± 10.39	0.81 ± 0.14	107.26 ± 15.84	0.93 ± 0.12	574.59 ± 44.38	1.17 ± 0.24
	323	128.07 ± 13.04	0.96 ± 0.05	102.99 ± 20.78	1.18 ± 0.14	560.36 ± 19.36	1.45 ± 0.14
20 wt % Zeolite A/ PTMSP	298	105.74 ± 31.71	25.57 ± 11.67	159.50 ± 21.05	3.70 ± 1.04	1251.40 ± 159.57	7.06 ± 0.76
	308	119.71 ± 23.13	27.74 ± 9.82	176.51 ± 4.18	3.41 ± 0.84	1455.17 ± 48.76	6.90 ± 0.81
	313	149.07 ± 31.80	47.45 ± 13.90	202.77 ± 14.76	3.64 ± 1.02	1529.29 ± 47.71	7.12 ± 1.18
	323	212.58 ± 12.69	43.59 ± 3.53	334.16 ± 19.65	5.03 ± 0.89	1589.47 ± 33.74	7.15 ± 0.15

Since permeance is the ratio of permeability and layer thickness, the thinner the skin layer, the higher the permeance [25, 50]. In the case of IL-CS-based membranes, the CO_2 permeance at 298 K increases from 8.49 GPU in the dense homogeneous flat form up to 102 GPU and 4226 GPU in composite flat and composite HF configuration, respectively. This enhancement is maintained, in the same proportion, in all the temperature ranges studied. Furthermore, HKUST-1/IL-CS, PTMSP, and zeolite A/PTMSP membranes also present this increment of the CO_2 permeance up to two orders of magnitude.

Liu et al. [53] observed for semi-crystalline PEBA/PSf composite membranes that the temperature increase reduced the significance of plasticization, at the low pressure of CO_2 capture from flue gas in post-combustion processes [54].

Regarding selectivity, only in the IL-CS and HKUST-1/IL-CS membranes, the selectivity approaches the intrinsic selectivity of dense homogeneous flat membranes, so one can expect that a defect-free thin selective layer has been obtained in these cases.

In the case of PTMSP-based membranes, the selectivity and thermal stability of zeolite A/PTMSP MMMs was greatly improved in self-standing dense homogeneous membranes [15], but not transferred to flat composite or HF geometries because of lower compatibility between the particles and the polymer matrix than in the CS-based membranes, leading to the formation of pinholes. In both cases, the selectivity is still too low to be considered as membranes for CO_2 separation in post-combustion processes, but the higher thermal stability, easy fabrication method, and reproducibility give scope for these membranes to be used as membrane contactors in CO_2 desorption at elevated temperatures [55].

Figs. 4 and 5 display Arrhenius plots of the PTMSP-based and IL-CS-based composite membranes in flat and HF geometries as a function of temperature. A good correlation is observed in all cases ($R^2 = 0.94 \pm 0.06$), i.e., the effect of temperature on gas permeance is well described in terms of an Arrhenius expression. Ji et al. [8] and Chen et al. [56] studied the effect of temperature on CO_2 post-combustion separation for polymer-blend composite HF membranes and found that gas permeance increased with higher temperature. Fig. 4 a demonstrates how the Arrhenius trend is followed by pure PTMSP unsupported and composite membranes, while Fig. 4 b presents an opposite effect of temperature in the permeance of zeolite A/PTMSP-based membranes.

The influence of temperature on zeolite A/PTMSP composite membranes is opposite to that of pure PTMSP composite membranes, as observed in dense homogeneous flat morphology [15]. In general, the composite MMMs show activated diffusion transport mechanism by the effect of porous zeolite within the selective layer [57].

Fig. 5 a illustrates the effect of temperature of IL-CS-based membranes and Fig. 5 b the behavior of HKUST-1/IL-CS-based membranes with temperature. The temperature influence on IL-CS membranes is almost negligible (Fig. 5 a) as reported for the dense homogeneous flat form [19]. The porous HKUST-1

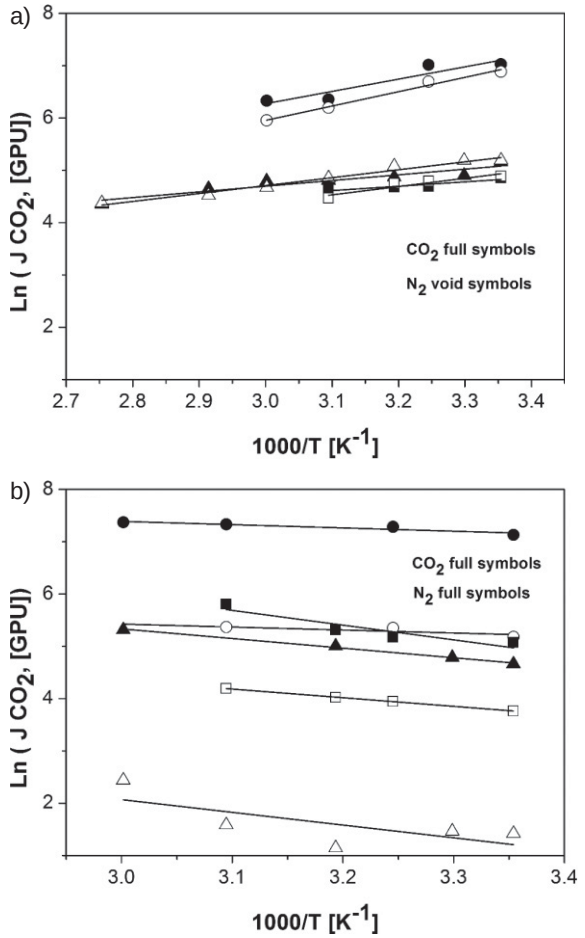

Figure 4. Arrhenius relationship of the dense homogeneous flat (triangles), composite flat (squares), and CHF membranes (circles) with temperature. (a) Pure PTMSP selective layer, (b) 20 wt % zeolite A/PTMSP selective layer.

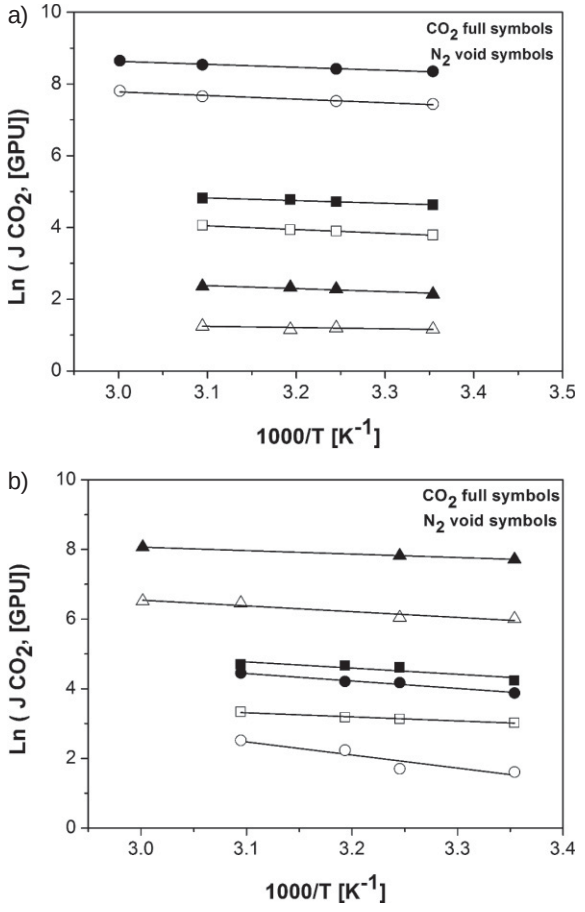

Figure 5. Arrhenius relationships of the dense homogeneous flat (triangles), composite flat (squares), and CHF membranes (circles) with temperature. (a) IL-CS, (b) 5 wt % HKUST-1/IL-CS coated layer.

filler seems also to provide a slight activation with temperature, as observed for the dense homogeneous flat configuration [29]. In the latter case, the impact of temperature on composite membranes is not changed with respect to the self-standing membrane configuration. When each temperature permeation cycle was finished, an additional experiment was repeated at 298 K to check that the performance was the same as before, to guarantee that the integrity of the membrane is maintained [58].

The activation energies for permeation through the different membranes and configurations are presented in Tab. 5. In pure PTMSP-based membranes, the activation energy for permeation is negative, as reported for glassy polyimides where the influence of solubility in permeation is significant [13, 59]. This has been also observed for P84 HF membranes [60]. In the case of the composite MMMs studied in this work, the activation energies have positive values.

On the one hand, the increase of activation energies for permeation means that an interaction phenomenon occurs between the dispersed zeolite fillers and the PTMSP matrix [15, 27, 43]. For the zeolite A/PTMSP-based membranes, the activation energies of permeation are positive in the three configurations. Whereas the activation energies of the zeolite A/PTMSP flat composite membranes are similar to those of dense homogeneous self-standing configuration, the activation energies of the CHF membrane slightly decreases. On the other hand, for IL-CS-based membranes as well as HKUST-1/IL-CS membranes, the activation energies are very similar in the three membrane configurations. However, the activation energies of the IL-CS dense homogeneous membranes were positive and had low values because the IL enhances the CO_2 affinity of the membrane material and reduces the influence of temperature in diffusivity and, therefore, in permeability [19].

In HKUST-1/IL-CS MMMs, the temperature influence in the CO_2/N_2 separation performance increases slightly as was commented above. Consequently, the activation energies of HKUST-1/IL-CS MMMs are higher than those of IL-CS membranes in Tab. 5, regardless the configuration. This could be attributed to the good adhesion and compatibility between IL, porous HKUST-1 nanoparticles, CS matrix, and PSf support. In general, the permeability through the MMM presented in this work decreases with lower temperature, and the activation energy of permeation is positive [25]. Raising the temperature increases the

Table 5. CO_2 and N_2 activation energies obtained for the different membranes and configurations studied in this work.

Selective membrane material	Support	Configuration	E_a CO_2 [kJ mol^{-1}]	E_a N_2 [kJ mol^{-1}]
–	PES	Flat	8.31 ± 2.85	5.41 ± 1.06
	PSf	HF	9.24 ± 0.68	9.43 ± 0.15
	P84	HF	−6.85 ± 1.56	−8.04 ± 2.41
PTMSP	–	Dense homogeneous flat	−9.07 ± 1.35	−12.64 ± 3.33
	PES	composite flat	−7.00 ± 3.57	−13.13 ± 3.22
	P84	composite HF	−19.62 ± 5.27	−22.81 ± 1.26
20 wt % ZeoliteA/ PTMSP	–	Dense homogeneous flat	15.34 ± 4.41	20.21 ± 7.96
	PES	Composite flat	23.39 ± 3.78	13.78 ± 4.57
	P84	Composite HF	5.28 ± 1.15	1.54 ± 0.62
IL-CS	–	Dense homogeneous flat	7.09 ± 2.68	2.78 ± 0.13
	PES	Composite flat	6.20 ± 1.15	8.48 ± 2.12
	PSf	Composite HF	6.87 ± 2.94	8.44 ± 2.16
5 wt % HKUST-1/IL-CS	–	Dense homogeneous flat	17.88 ± 3.12	31.22 ± 4.86
	PES	Composite flat	14.77 ± 4.51	9.92 ± 2.87
	PSf	Composite HF	8.29 ± 0.64	13.67 ± 4.42

kinetic energy of gas molecules as well as mobility of the polymer chains and enhances the gases' permeation flux [61].

4 Conclusions

The effect of the change of geometry of a highly CO_2/N_2-permselective and thermally resistant self-standing MMM to composite flat and composite HF configuration is important for the scalability of MMM fabrication. In this work, composite MMMs were prepared by dip-coating the highly CO_2/N_2-permselective MMM materials developed in our laboratory on selected compatible porous supports of flat and HF geometries. The drying procedure and post-treatment previously optimized for dense homogeneous flat MMMs was applied to the composite membrane preparation.

The number of coatings and viscosity of the coating solutions were taken into account to obtain a thin layer of the novel material and prevent penetration of the support. The composite flat and HF membrane fabrication procedure developed was reproducible. SEM images reveal that a homogeneous thin layer was formed on top of the porous support along the whole membrane area regardless the geometry. The thicknesses of HKUST-1/IL-CS and IL-CS composite membranes were reduced down 97 % from flat to HF morphologies. The selective layer thickness of pure PTMSP and zeolite A/PTMSP composite MMMs was reduced by 90 % and 85 % from flat and HF geometries, respectively.

The membranes were tested by CO_2 and N_2 gas permeation performance in the temperature range 298–333 K. In all cases, the selective MMM layer thickness reductions also led to an important increase of the CO_2 permeance of more than one or two orders of magnitude for composite flat and HF configuration, respectively. The IL-CS and HKUST/IL-CS composite MMMs exhibited increased permeation flux and similar CO_2/N_2 selectivity, even with higher temperature, and this permselectivity was correlated with the lower thickness of the selective MMM layer.

The effect of temperature on gas separation performance was similar for the IL-CS and HKUST-1/IL-CS composite membranes and the dense homogeneous unsupported membranes. The activation energies of composite MMMs are positive, regardless the composition and geometrical configuration. Although the selectivity is still low to be considered as CO_2-selective membranes, the high thermal stability of the novel composite MMMs may have potential as membrane contactors for CO_2 desorption in post-combustion capture, which can be addressed in a future work.

Acknowledgment

Financial support from the Spanish Ministry of Economy and Competitiveness (MINECO) under project CTQ2012-31229 at the Universidad de Cantabria is gratefully acknowledged. A.F.B. and C.C.C. also thank the MINECO for the Early Stage Researcher (BES2013-064266) and "Ramón y Cajal" (RYC2011-0855) contracts, respectively. The authors thank F. Noboru Ramirez-Matsumoto for his contribution in the synthesis and permeation experiments of the CS and IL-CS composite flat membranes by the modified IP method.

The authors have declared no conflict of interest.

Symbols used

J	[GPU]	permeance
l_i	[μm]	thickness
P	[Barrer]	permeability

Greek letters

α	[–]	ideal selectivity
η	[mPa s]	viscosity

Abbreviations

CHF	composite hollow-fiber
CS	chitosan
FE-SEM	field electron scanning microscopy
HF	hollow fiber
IL	ionic liquid
IL/CS	[emim][Ac]/chitosan
IP	interfacial polymerization
MMM	mixed-matrix membrane
PDMS	poly(dimethylsiloxane)
PES	polyethersulfone
PI	polyimide
Psf	polysulfone
PTMSP	poly(1-trimethylsilyl-1-propyne)
SPES	sulfonated polyethersulfone
TMC	trimesoyl chloride
UF	ultrafiltration

References

[1] J. C. Abanades, B. Arias, A. Lyngfelt, T. Mattisson, D. E. Wiley, H. Li, M. T. Ho, E. Mangano, S. Brandani, *Int. J. Greenhouse Gas Control* **2015**, *40*, 126–166.

[2] L. M. Robeson, *J. Membr. Sci.* **2008**, *320*, 390–400. DOI: 10.1016/j.memsci.2008.04.030

[3] A. S. Bhown, *Energy Procedia* **2014**, *63*, 542–549. DOI: 10.1016/j.egypro.2014.11.059

[4] M. Rezakazemi, A. Ebadi Amooghin, M. M. Montazer-Rahmati, A. F. Ismail, T. Matsuura, *Prog. Polym. Sci.* **2014**, *39*, 817–861. DOI: 10.1016/j.progpolymsci.2014.01.003.

[5] T. S. Chung, L. Y. Jiang, Y. Li, S. Kulprathipanja, *Prog. Polym. Sci.* **2007**, *32*, 483–507. DOI: 10.1016/j.progpolymsci.2007.01.008

[6] R. Mahajan, R. Burns, M. Schaeffer, W. J. Koros, *J. Appl. Polym. Sci.* **2002**, *86*, 881–890. DOI: 10.1002/app.10998

[7] U. Beuscher, C. H. Gooding, *J. Membr. Sci.* **1997**, *132*, 213–227. DOI: 10.1016/S0376-7388(97)00071-9

[8] P. Ji, Y. Cao, H. Zhao, G. Kang, X. Jie, D. Liu, J. Liu, Q. Yuan, *J. Membr. Sci.* **2009**, *342*, 190–197. DOI: 10.1016/j.memsci.2009.06.038

[9] A. K. Zulhairun, Z. G. Fachrurrazi, M. Nur Izwanne, A. F. Ismail, *Sep. Purif. Technol.* **2015**, *146*, 85–93. DOI: 10.1016/j.seppur.2015.03.033

[10] C. Zhang, K. Zhang, L. Xu, Y. Labreche, B. Kraftschik, W. J. Koros, *AIChE J.* **2014**, *60*, 2625–2635. DOI: 10.1002/aic.14496

[11] N. Peng, N. Widjojo, P. Sukitpaneenit, M. M. Teoh, G. G. Lipscomb, T. S. Chung, J. Y. Lai, *Prog. Polym. Sci.* **2012**, *37*, 1401–1424. DOI: 10.1016/j.progpolymsci.2012.01.001

[12] M. Sandru, S. H. Haukebø, M. B. Hägg, *J. Membr. Sci.* **2010**, *346*, 172–186. DOI: 10.1016/j.memsci.2009.09.039

[13] T. C. Merkel, R. P. Gupta, B. S. Turk, B. D. Freeman, *J. Membr. Sci.* **2001**, *191*, 85–94. DOI: 10.1016/S0376-7388(01)00452-5

[14] A. Morisato, H. C. Shen, S. S. Sankar, B. D. Freeman, I. Pinnau, C. G. Casillas, *J. Polym. Sci., Part B: Polym. Phys.* **1996**, *34*, 2209–2222. DOI: 10.1002/(SICI)1099-0488(19960930)34

[15] A. Fernández-Barquín, C. Casado-Coterillo, M. Palomino, S. Valencia, A. Irabien, *Chem. Eng. Technol.* **2015**, *38*, 658–666. DOI: 10.1002/ceat.201400641

[16] M. Palomino, A. Corma, F. Rey, S. Valencia, *Langmuir* **2010**, *26*, 1910–1917. DOI: 10.1021/la9026656

[17] L. Liu, A. Chakma, X. Feng, *J. Membr. Sci.* **2008**, *310*, 66–75. DOI: 10.1016/j.memsci.2007.10.032

[18] Z. Dai, R. D. Noble, D. L. Gin, X. Zhang, L. Deng, *J. Membr. Sci.* **2016**, *497*, 1–20. DOI: 10.1016/j.memsci.2015.08.060

[19] E. Santos, E. Rodríguez-Fernández, C. Casado-Coterillo, Á. Irabien, *Int. J. Chem. React. Eng.* **2015**, *14 (3)*, 713–718. DOI: 10.1515/ijcre-2014-0109

[20] S. B. Carruthers, G. L. Ramos, W. J. Koros, *J. Appl. Polym. Sci.* **2003**, *90*, 399–411. DOI: 10.1002/app.12623

[21] W. J. Koros, R. Mahajan, *J. Membr. Sci.* **2000**, *175*, 181–196. DOI: 10.1016/S0376-7388(00)00418-X

[22] C. Y. Feng, K. C. Khulbe, T. Matsuura, A. F. Ismail, *Sep. Purif. Technol.* **2013**, *111*, 43–71. DOI: 10.1016/j.seppur.2013.03.017

[23] J. K. Adewole, *J. Appl. Polym. Sci.* **2016**, *133*, 43606–43614. DOI: 10.1002/app.43606

[24] J. C. Jansen, M. G. Buonomenna, A. Figoli, E. Drioli, *J. Membr. Sci.* **2006**, *272*, 188–197. DOI: 10.1016/j.memsci.2005.07.036

[25] L. Liu, E. S. Sanders, J. R. Johnson, O. Karvan, S. Kulkarni, D. J. Hasse, W. J. Koros, *J. Membr. Sci.* **2013**, *446*, 433–439. DOI: 10.1016/j.memsci.2013.06.001

[26] B. W. Rowe, L. M. Robeson, B. D. Freeman, D. R. Paul, *J. Membr. Sci.* **2010**, *360*, 58–69. DOI: 10.1016/j.memsci.2010.04.047

[27] A. Fernández-Barquín, C. Casado-Coterillo, M. Palomino, S. Valencia, A. Irabien, *Sep. Purif. Technol.* **2016**, *157*, 102–111. DOI: 10.1016/j.seppur.2015.11.032

[28] C. Casado-Coterillo, M. M. López-Guerrero, A. Irabien, *Membranes* **2014**, *4*, 287–301. DOI: 10.3390/membranes4020287

[29] C. Casado-Coterillo, A. Fernández-Barquín, B. Zornoza, C. Téllez, J. Coronas, A. Irabien, *RSC Adv.* **2015**, *5*, 102350–102361. DOI: 10.1039/c5ra19331a

[30] S. Sridhar, B. Smitha, S. Mayor, B. Prathab, T. M. Aminabhavi, *J. Mater. Sci.* **2007**, *42*, 9392–9401. DOI: 10.1007/s10853-007-1813-5

[31] S. Veríssimo, K.-V. Peinemann, J. Bordado, *J. Membr. Sci.* **2005**, *264*, 48–55. DOI: 10.1016/j.memsci.2005.04.020

[32] M. Etxeberria, P. Corengia, S. Miguel, J. Zuniga, E. Fernandez-Gesalaga, P. Jimenez, *Proc. Eng.* **2012**, *44*, 791–792. DOI: 10.1016/j.proeng.2012.08.573

[33] L. Gomez-Coma, A. Garea, J. C. Rouch, T. Savart, J. F. Lahitte, J. C. Remigy, *J. Membr. Sci.* **2016**, *498*, 218–226. DOI: 10.1016/j.memsci.2015.10.023

[34] A. Jamil, O. P. Ching, A. B. M. Shariff, *Chem. Eng. Technol.* **2016**, *39*, 1393–1405. DOI: 10.1002/ceat.201500395

[35] M. F. A. Wahab, A. F. Ismail, S. J. Shilton, *Sep. Purif. Technol.* **2012**, *86*, 41–48. DOI: 10.1016/j.seppur.2011.10.018

[36] S. S. Madaeni, M. M. S. Badieh, V. Vatanpour, *Polym. Eng. Sci.* **2013**, *53*, 1878–1885. DOI: 10.1002/pen.23456

[37] T. S. Chung, S. K. Teoh, X. Hu, *J. Membr. Sci.* **1997**, *133*, 161–175. DOI: 10.1016/S0376-7388(97)00101-4

[38] F. Cacho-Bailo, G. Caro, M. Etxeberría-Benavides, O. Karvan, C. Téllez, J. Coronas, *RSC Adv.* **2016**, *6*, 5881–5889. DOI: 10.1039/c5ra26076k

[39] J. N. Barsema, G. C. Kapantaidakis, N. F. A. Van Der Vegt, G. H. Koops, M. Wessling, *J. Membr. Sci.* **2003**, *216*, 195–205. DOI: 10.1016/S0376-7388(03)00071-1

[40] P. S. Tin, T. S. Chung, Y. Liu, R. Wang, *Carbon* **2004**, *42*, 3123–3131. DOI: 10.1016/j.carbon.2004.07.026

[41] M. P. Chenar, M. Soltanieh, T. Matsuura, A. Tabe-Mohammadi, C. Feng, *Sep. Purif. Technol.* **2006**, *51*, 359–366. DOI: 10.1016/j.seppur.2006.02.018

[42] M. Kattula, K. Ponnuru, L. Zhu, W. Jia, H. Lin, E. P. Furlani, *Sci. Rep.* **2015**, *5*, 1–9. DOI: 10.1038/srep15016

[43] J. Qiu, J. M. Zheng, K. V. Peinemann, *Macromolecules* **2006**, *39*, 4093–4100. DOI: 10.1021/ma0603635

[44] E. Lasseuguette, J. C. Rouch, J. C. Remigy, *Ind. Eng. Chem. Res.* **2013**, *52*, 13146–13158. DOI: 10.1021/ie401874m

[45] H. Z. Chen, Z. Thong, P. Li, T.-S. Chung, *Int. J. Hydrogen Energy* **2014**, *39*, 5043–5053. DOI: 10.1016/j.ijhydene.2014.01.047

[46] P. D. Sutrisna, J. Hou, H. Li, Y. Zhang, V. Chen, *J. Membr. Sci.* **2017**, *524*, 266–279. DOI: 10.1016/j.memsci.2016.11.048

[47] K. T. Woo, J. Lee, G. Dong, J. S. Kim, Y. S. Do, W. S. Hung, K. R. Lee, B. Barbieri, E. Drioli, Y. M. Lee, *J. Membr. Sci.* **2015**, *490*, 129–138. DOI: 10.1016/j.memsci.2015.04.059

[48] E. Esposito, G. Clarizia, P. Bernardo, J. C. Jansen, Z. Sedlakova. P. Izak, S. Curcio, B. de Cindio, F. Tasselli, *Chem. Eng. Process. Process Intensif.* **2015**, *94*, 53–61. DOI: 10.1016/j.cep.2015.03.016

[49] H. Z. Chen, Z. Thong, P. Li, T. S. Chung, *Int. J. Hydrogen Energy* **2014**, *39*, 5043–5053. DOI: 10.1016/j.ijhydene.2014.01.047

[50] T. He, M. H. V. Mulder, H. Strathmann, M. Wessling, *J. Membr. Sci.* **2002**, *207*, 143–156. DOI: 10.1016/S0376-7388(02)00118-7

[51] Y. L. Liu, C. H. Yu, L. C. Ma, G. C. Lin, H. A. Tsai, J. Y. Lai, *J. Membr. Sci.* **2008**, *311*, 243–250. DOI: 10.1016/j.memsci.2007.12.040

[52] T. Kai, T. Kouketsu, S. Duan, S. Kazama, K. Yamada, *Sep. Purif. Technol.* **2008**, *63*, 524–530. DOI: 10.1016/j.seppur.2008.06.012

[53] A. Mondal, B. Mandal, *J. Membr. Sci.* **2013**, *446*, 383–394. DOI: 10.1016/j.memsci.2013.06.052

[54] L. Liu, A. Chakma, X. Feng, *Chem. Eng. J.* **2004**, *105*, 43–51. DOI: 10.1016/j.cej.2004.08.005

[55] G. A. Dibrov, V. V. Volkov, V. P. Vasilevsky, A. A. Shutova, S. D. Bazhenov, V. S. Khotimsky, A. van de Runstraat, E. L. V. Goetheer, A. V. Volkov, *J. Membr. Sci.* **2014**, *470*, 439–450. DOI: 10.1016/j.memsci.2014.07.056

[56] C. C. Chen, W. Qiu, S. J. Miller, W. J. Koros, *J. Membr. Sci.* **2011**, *382*, 212–221. DOI: 10.1016/j.memsci.2011.08.015

[57] Y. Dai, J. R. Johnson, O. Karvan, D. S. Sholl, W. J. Koros, *J. Membr. Sci.* **2012**, *401–402*, 76–82. DOI: 10.1016/j.memsci.2012.01.044

[58] C. I. Chaidou, G. Pantoleontos, D. E. Koutsonikolas, S. P. Kaldis, G. P. Sakellaropoulos, *Sep. Sci. Technol.* **2012**, *47*, 950–962. DOI: 10.1080/01496395.2011.645263

[59] Y. P. Yampolskii, N. E. Kaliuzhnyi, S. G. Durgarjan, *Macromolecules* **1986**, *19*, 846–850. DOI: 10.1021/ma00157a062

[60] E. P. Favvas, K. L. Stefanopoulos, J. W. Nolan, S. K. Papageorgiou, A. C. Mitropoulos, D. Lairez, *Sep. Purif. Technol.* **2014**, *132*, 336–345. DOI: 10.1016/j.seppur.2014.05.013

[61] Y. Dai, X. Ruan, F. Bai, M. Yu, H. Li, Z. Zhao, G. He, *Appl. Surf. Sci.* **2016**, *360*, 164–173. DOI: 10.1016/j.apsusc.2015.11.014